

Laboratory experiments on dynamo action and magnetically triggered flow instabilities

F. STEFANI^{*†}, A. GAILITIS[‡], G. GERBETH[†], A. GIESECKE[†],
Th. GUNDRUM[†], G. RÜDIGER[§], M. SEILMAYER[†], T. VOGT[†]

March 12, 2018

[†]Helmholtz-Zentrum Dresden-Rossendorf, Bautzner Landstr. 400, D-01328 Dresden, Germany

[‡]Institute of Physics, Latvian University, LV-2169 Salaspils 1, Riga, Latvia

[§]Leibniz-Institut für Astrophysik Potsdam, An der Sternwarte 16, D-14467 Potsdam, Germany

Magnetic fields of planets, stars and galaxies are generated by self-excitation in moving electrically conducting fluids. Once produced, magnetic fields can play an active role in cosmic structure formation by destabilizing rotational flows that would be otherwise hydrodynamically stable. For a long time, both hydromagnetic dynamo action as well as magnetically triggered flow instabilities had been the subject of purely theoretical research. Meanwhile, however, the dynamo effect has been observed in large-scale liquid sodium experiments in Riga, Karlsruhe and Cadarache. In this paper, we summarize the results of liquid metal experiments devoted to the dynamo effect and various magnetic instabilities such as the helical and the azimuthal magnetorotational instability and the Tayler instability. We discuss in detail our plans for a precession-driven dynamo experiment and a large-scale Tayler-Couette experiment using liquid sodium, and on the prospects to observe magnetically triggered instabilities of flows with positive shear.

Keywords: Dynamo; Instabilities

1 Introduction

Self-excitation in moving electrically conducting fluids, i.e. hydromagnetic dynamo action, is well-known to be responsible for the generation of planetary, stellar and galactic magnetic fields (Rüdiger *et al.* 2013). Yet, cosmic magnetic fields, rather than being only passive by-products of fluid motion, play also an active role in the formation of stars and black-holes by fostering angular momentum transport and mass accretion via the magnetorotational instability (MRI) (Balbus 2003). Complementary to theoretical and numerical modeling of these fundamental problems of geo- and astrophysical magnetohydrodynamics (MHD), the last two decades have seen great progress in respective experimental studies (Gailitis *et al.* 2002, Stefani *et al.* 2008, Lathrop and Forest 2011). By now, the "magic" threshold for magnetic field self-excitation has been attained in three large-scale liquid sodium experiments in Riga (Gailitis *et al.* 2000, 2003, 2004), Karlsruhe (Müller

*Corresponding author. Email: F.Stefani@hzdr.de

and Stieglitz 2000, Stieglitz and Müller, 2001, Müller *et al.* 2004), and Cadarache (Monchaux *et al.* 2007, Monchaux *et al.* 2009, Miralles *et al.* 2013). Dynamo and MRI related liquid metal experiments were carried out, or are under construction, all over the world, e.g. in Madison (Spence *et al.* 2006), Maryland (Zimmerman *et al.* 2010), Socorro (Colgate *et al.* 2011), Princeton (Nornberg *et al.* 2010), Perm (Frick *et al.* 2010), Grenoble (Schmitt *et al.* 2013), and Zürich (Hollerbach *et al.* 2013). An MRI-like coherent structure of velocity and magnetic fields had been observed in a liquid sodium spherical Couette flow at the University of Maryland (Sisan *et al.* 2004), albeit on the background of an already turbulent flow. Both the helical (HMRI) and the azimuthal (AMRI) versions of MRI were observed and explored in much detail in the experiment PROMISE at Helmholtz-Zentrum Dresden-Rossendorf (HZDR) (Stefani *et al.* 2006, Stefani *et al.* 2009, Seilmayer *et al.* 2014). The current-driven, kink-type Tayler instability (TI) (Tayler 1973), which is at the root of an alternative model of the solar dynamo (Spruit 2002), was demonstrated in a long column of a liquid metal, just by running a strong electrical current through it (Seilmayer *et al.* 2012).

More often than not, the need to design and optimize those experiments, and to understand their occasionally unexpected results, has incited complementary theoretical and numerical work, which in some cases also spurred new discussions in the original geo- or astrophysical domain. Moreover, the experiments have triggered the development of flow measuring techniques also applicable to steel casting and crystal growth, e.g. Contactless Inductive Flow Tomography (CIFT) (Wondrak *et al.* 2010), and of various stabilization methods for large-scale liquid metal batteries (Stefani *et al.* 2016a).

The first objective of this paper is to provide a cursory, incomplete, and personally biased account of those previous experiments that were devoted to dynamo action and magnetically triggered flow instabilities. Then, we will discuss in more detail the plans for three new liquid sodium experiments. These comprise, first, a truly homogeneous dynamo in form of a large-scale precession experiment. Besides thermal and compositional buoyancy, precession has long been discussed as an alternative, or at least additional, power source of the geodynamo (Malkus 1968, Kerswell 1993, Tilgner 2005, Tilgner 2007, Wu and Roberts 2009, Shalimov 2006), the ancient lunar dynamo (Dwyer *et al.* 2011, Noir and Cebon 2013, Weiss and Tikoo 2014), or the asteroid Vesta (Fu *et al.* 2002). The second experiment will deal with different versions of the MRI, and their combinations with the TI, with the main goal to find the "holy grail" of this research field, which is standard MRI (SMRI) with a purely axial field being applied (Velikhov 1959, Balbus and Hawley 1991). Third, we will discuss a possible experimental demonstration of the recent prediction that rotational flows with a radially increasing angular velocity, such as it prevails in an equator-near-strip of the solar tachocline, might be destabilized by purely azimuthal magnetic fields (Stefani and Kirillov 2015, Rüdiger *et al.* 2016, Rüdiger *et al.* 2018).

All these experiments will be carried out in frame of the liquid sodium platform DRES-DYN (DREsden Sodium facility for DYNamo and thermohydraulic studies) at HZDR (Stefani *et al.* 2012, Stefani *et al.* 2015), whose building construction has been finalized in 2017.

2 Previous experiments

In this section, we briefly summarize the previous experiments on dynamo action and various magnetically triggered flow instabilities. For more details, see the survey papers by Gailitis *et al.* (2002), Stefani *et al.* (2008), and Lathrop and Forest (2011).

2.1 Dynamo (related) experiments

For many decades, it had been a dream to simulate a homogenous, near-natural dynamo in the laboratory. In the 1960ies, based on Herzenberg's theoretical derivation of a working dynamo (Herzenberg 1958), Lowes and Wilkinson (1963,1967) conducted a series of quasi-homogeneous dynamo experiments consisting of two or more rotating soft-iron cylinders embedded into blocks of the same material. These experiments suffered from the hysteresis effect of the used magnetic material, and from the rigidity of their construction which made the saturation mechanism very unlike to that of a fluid dynamo. However, their step-by-step improvement even led to a sort of reversals similar to those of the geomagnetic field (Wilkinson 1984), for whose explanation the oscillatory solutions of Herzenberg's dynamo, as first found by Gailitis (1973), might play a role.

Proposed by Steenbeck, a liquid sodium experiment with two orthogonally interlaced copper channels was carried out in 1967. Reaching flow velocities of up to 11 m/s, this experiment provided clear evidence of the α -effect, i.e. of the induction of an electromotive force *parallel* to the applied magnetic field (Steenbeck *et al.* 1967). Due to its relevance in our context, we mention the precession experiment with liquid sodium reported by Gans (1971). The sodium was enclosed in a cylindrical volume of 25 cm diameter and approximately the same height. Rather high rotation rates of up to 60 Hz were attained, but the precession rate was quite low (below 1 Hz). Nevertheless, Gans was able to measure a magnetic field amplification by a factor of 3. A wealth of knowledge on precession driven flows has been gained with water experiments in various geometries (Malkus 1967, Vanyo and Dunn 2002, Lagrange *et al.* 2008, Mouhali *et al.* 2012, Goto *et al.* 2014, Lin *et al.* 2015). With the cylindrical water experiment at HZDR (see Figure 4f further below), the hysteretic character of the laminar-turbulent transition was characterized in much detail (Herault *et al.* 2015).

Based on the theoretical work of Ponomarenko (1973), and on further optimization by Gailitis and Freibergs (1976), an early version of the later Riga dynamo experiment was carried out in 1987 (Gailitis 1987). After having reached a significant amplification of an applied magnetic field, the experiment had to be stopped due to technical problems. The very Riga dynamo, whose ultimate success relied on the iterative optimization of the flow profile (Stefani *et al.* 1999), became operative in November 1999. Besides the strong amplification of an externally applied field (up to a factor 25), we finally observed a slowly growing magnetic eigenfield, i.e. a kinematic dynamo, but for only 15 seconds (Gailitis *et al.* 2000), after which the maximal rotation rate had to be reduced for safety reasons. In July 2000, the saturated regime of this dynamo was also reached (Gailitis *et al.* 2001). Since that time, 10 experimental campaigns haven been carried out (Gailitis *et al.* 2018), the last ones in June 2016 (Gailitis and Lipsbergs 2017) and April 2017, with an ever increasing refinement of measurement techniques. Figure 1 shows, together with a sketch of the facility and a simulation of the magnetic eigenfield, a compilation of the

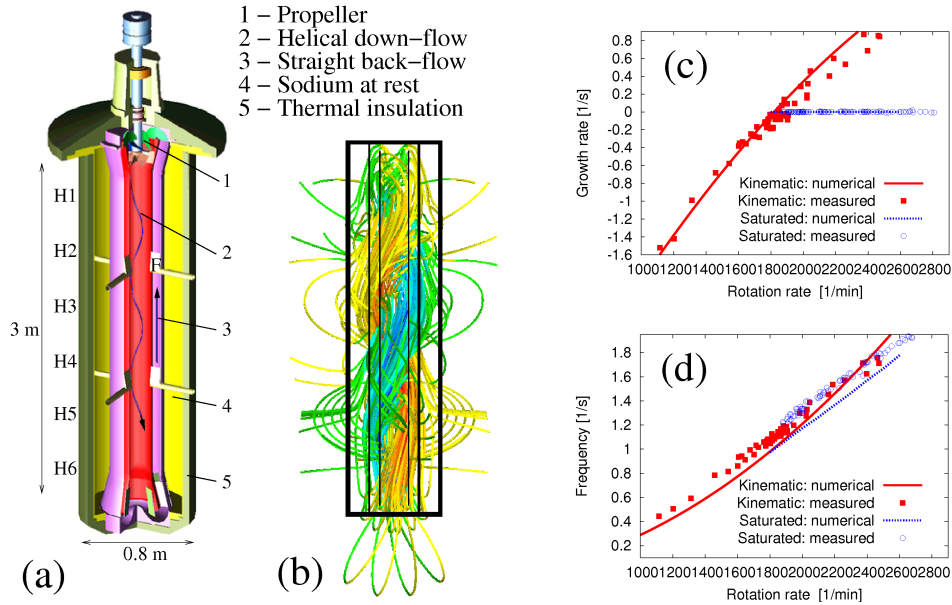


Figure 1: The Riga dynamo experiment. (a) Scheme. (b) Simulated magnetic eigenfield in form of a double helix structure that rotates around the vertical axis with a frequency between 1 and 2 Hz. Experimentally determined and numerically computed growth rates (c) and frequencies (d), both in the kinematic and in the saturated regime of the dynamo (after Gailitis *et al.* 2009).

main results in form of the experimentally and numerically determined growth rates and eigenfrequencies, both in the kinematic and in the saturated regime.

Nearly simultaneously with the single-scale Riga facility, the two-scale dynamo experiment in Karlsruhe became operative and immediately provided self-excitation and saturation of a magnetic eigenfield (Müller and Stieglitz *et al.* 2000, Stieglitz and Müller 2001, Müller *et al.* 2004). Similar as in the Riga case, the results of this experiment were in nearly perfect agreement with numerical predictions (Rädler *et al.* 1998, Tilgner 2002, Rädler *et al.* 2002). More surprising were the results of the von-Kármán-sodium (VKS) dynamo experiment in Cadarache that reached the threshold of self-excitation in 2006 (Monchaux *et al.* 2007). The reasons for the discrepancy between the numerically predicted and the experimentally observed field topology are still a matter of ongoing research: the soft iron impellers seem to play a big role here, as discussed in a number of numerical simulations (Giasecke *et al.* 2010, Giasecke *et al.* 2012, Nore *et al.* 2015, Kreuzahler *et al.* 2017). This notwithstanding, the results of the VKS experiment are fascinating, in particular with view on its rich dynamical behaviour, including field reversals and excursions (Monchaux *et al.* 2009, Miralles *et al.* 2013).

By now, dynamo (related) experiments are carried out at many places in the world (Stefani *et al.* 2008, Lathrop and Forest 2011). Among their most important results are the observation of an unexpected axi-symmetric induced field at the dynamo experiment in Madison (Spence *et al.* 2006), the accurate determination of a turbulence-enhanced resistivity in Perm (Frick *et al.* 2010), the identification of an MRI-like mode in a turbulent spherical Couette flow in Maryland (Sisan *et al.* 2004), the measurement of a strong Ω -

effect in Socorro (Colgate *et al.* 2011), and the observation of the numerically predicted super-rotation at the rotating sphere experiment in Grenoble (Schmitt *et al.* 2013). The rapidly rotating liquid sodium experiment in Zurich, with a radial electrical current and an imposed axial magnetic field, will allow to study the magnetostrophic regime (Hollerbach *et al.* 2013). And the old dream of a homopolar disk dynamo might finally come true in an experiment in Querétaro (Mexico) which uses an optimized system of a spirally slotted copper disk and liquid metal contacts (Avalos-Zuñiga *et al.* 2017).

2.2 Experiments on magnetically triggered flow instabilities

The preparatory decade of the first liquid sodium dynamo experiments concurred with the recognition of the fundamental importance of the MRI for accretion disk physics (Balbus and Hawley 1991, Balbus 2003). It soon became clear that the demonstration of SMRI, with a purely axial field being applied, would require similar experimental effort as dynamo experiments do (Rüdiger *et al.* 2003, Liu *et al.* 2006a). A corresponding experiment was constructed in Princeton and has shown interesting results on slow magneto-Coriolis waves (Nornberg *et al.* 2010) and on the magnetic destabilization of a free Shercliff layer (Roach *et al.* 2012), although not yet the very SMRI.

Since 2005 an experimental research programme has been pursued at HZDR which was devoted to the characterization of the helical (HMRI) and azimuthal version (AMRI) of the MRI in a Taylor-Couette flow with the eutectic metal GaInSn, which is liquid at room temperature and thus allows much simpler settings than liquid sodium experiments. The basic idea behind these PROMISE experiments (Stefani *et al.* 2006, Stefani *et al.* 2009, Seilmayer *et al.* 2014) is the fact that HMRI and AMRI work already at much lower values of the Reynolds (Re) and the Hartmann (Ha) number than SMRI (Hollerbach and Rüdiger 2005, Hollerbach *et al.* 2010). The reason for the different scaling behaviour of HMRI and SMRI is that SMRI represents a destabilized slow magneto-Coriolis wave, while HMRI is essentially a weakly destabilized inertial oscillation. Nevertheless, both instabilities are connected continuously (Hollerbach and Rüdiger 2005), a fact that was explained in terms of the appearance of an exceptional point where both modes coalesce and exchange their branches (Kirillov and Stefani 2010).

In a first version of this experiment (PROMISE 1), the appearance of the HMRI was already observed in the predicted window of Ha (Stefani *et al.* 2006, Stefani *et al.* 2007), starting from an axial current of around 4 kA. An imperfection of this first version was the strong influence of the Ekman pumping at the top and bottom lids which resulted in a radial jet (approximately at mid-height of the Taylor-Couette cell) where the MRI wave ceased to exist. To minimize this Ekman pumping the experiment was modified by installing end-rings that were split at a numerically optimized position (Szklański 2007). This version, PROMISE 2, is illustrated in Figure 2a. As a consequence of this apparently slight modification, the HMRI wave travelled throughout the entire height (Figure 2b) (Stefani *et al.* 2009), and the coincidence with numerical predictions became much better than in PROMISE 1 (see Figure 2c).

A third version, PROMISE 3, which required a significant enhancement of the power supply to provide central currents of up to 20 kA, has confirmed the numerical prediction of AMRI (Hollerbach *et al.* 2010). A peculiarity of this experiment was the surprisingly strong effect of the slight symmetry breaking of the applied field (owing to the one-sided

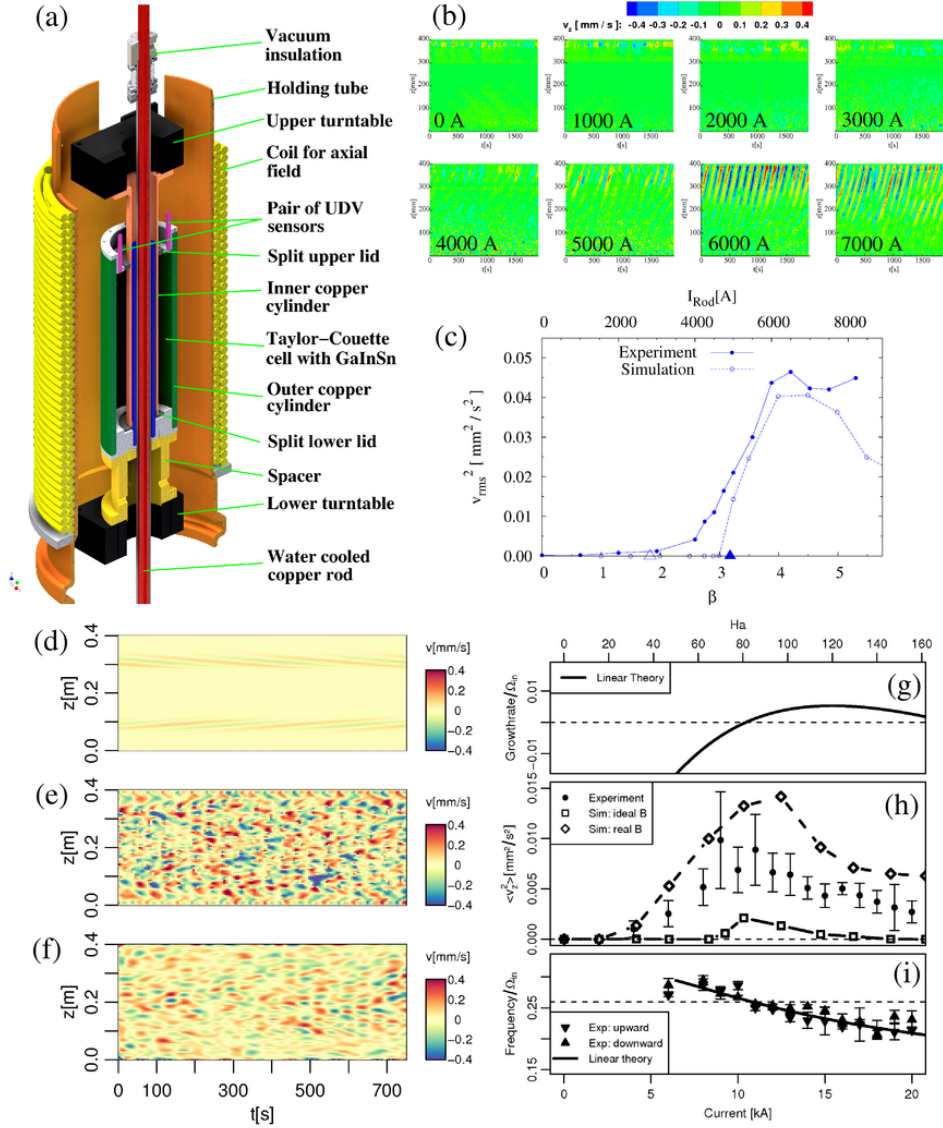


Figure 2: The PROMISE experiment at HZDR, and some of its main results on HMRI (b,c) and AMRI (d-i). (a) Sketch of the facility, comprising a Taylor-Couette cell with inner radius $r_i = 4$ cm, outer radius $r_o = 8$ cm, and a height $H = 40$ cm, filled with GaInSn, an external coil and a central copper rod for the generation of the axial and the azimuthal magnetic field, respectively. (b) Measured velocity structure when increasing the current through the central rod, for a fixed current of 76 A in the coil. Approximately at 5000 A, HMRI emerges as an upward travelling wave. (c) Experimentally and numerically determined dependence of the mean squared of the velocity perturbations on the applied rod current. Velocity perturbation $v_z(m = 1; z; t)$ for $Re = 1480$ and $Ha = 124$ for AMRI (after Seilmayer *et al.* 2014): (d) simulation for an idealized axisymmetric field. (e) Simulation for the realistic field geometry. (f) Measured velocity. (g) Numerically predicted growth rate. (h) Simulated and measured mean squared velocity perturbation. (i) Angular drift frequency.

wiring for the central current). While a perfectly symmetric field would have led to an instability pattern according to Figure 2d, the correct consideration of the symmetry breaking leads to the interpenetrating wave pattern as shown in Figure 2e, which was indeed observed in the experiment (Figure 2f). With improved numerics a reasonable agreement with the measured rms values (Figure 2h) and frequencies (Figure 2i) of the AMRI wave was achieved (Seilmayer *et al.* 2014).

Further to HMRI and AMRI, in another GaInSn experiment first evidence of the Taylor instability (TI) was gained, which expectedly set in at a current of around 3 kA running axially through a liquid metal column (Seilmayer *et al.* 2012).

3 The DRESDYN project

From the basic research viewpoint, the main aim of the DRESDYN project at HZDR is to contribute to a better understanding of the origin and the action of planetary, stellar, and galactic magnetic fields. Dedicated liquid sodium experiments will be carried out in parameter regions that are hardly accessible to numerics. Figure 3 gives some illustrations of the present status of the DRESDYN building, which is now ready to host the experiments.

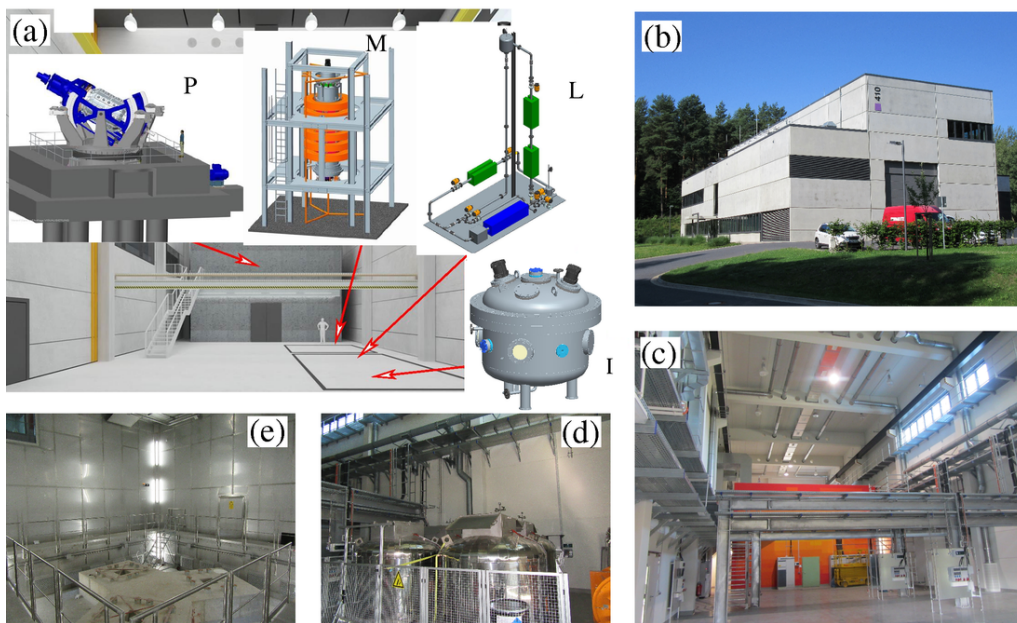


Figure 3: Overview about the DRESDYN facility and impressions of the building and infrastructure. (a) Scheme of the experimental hall with the major planned experiments: P - Precession experiment in a special containment, M - MRI/TI experiment, L - Sodium loop for testing measurement techniques, I - Sodium pool facility. (b) Finalized building from outside. (c) View into the experimental hall. (d) Containers for a total of 12 tons of sodium. (e) View into the safety containment with the massive ferro-concrete tripod for the precession experiment.

The basic studies in the frame of DRESDYN have three specific scientific goals: First,

to demonstrate magnetic field self-excitation in a truly homogeneous fluid, which is driven in a "natural" manner by precession. Second, to perform a combined MRI/TI experiment, with the particular aim to find the "holy grail" of demonstrating standard MRI, and third, to set-up and run an experiment on "Super-AMRI", which is supposed to confirm the surprising prediction of magnetic destabilization of rotating flows with positive shear. The large dimensions of the precession experiment (and, to some lesser extent, of the MRI/TI experiment, too) with several tons of liquid sodium, and its operation at the edge of technical feasibility, make DRESDYN a somewhat risky endeavor.

3.1 Precession dynamo

A mass of 6 tons of liquid sodium, set into motion only by the simultaneous rotation around two axes, without using any impellers or guiding blades, may indeed be considered *the* paradigm of a homogenous hydromagnetic dynamo. Precession has long been discussed as an energy source of the geodynamo (Malkus 1968, Kerswell 1993, Tilgner 2005, Tilgner 2007, Wu and Roberts 2009, Shalimov 2006, Nore *et al.* 2011, Goepfert and Tilgner 2016) and the ancient lunar dynamo (Dwyer *et al.* 2012, Noir and Cebbron 2013, Weiss and Tikoo 2014), and the link between various Milankovic cycles of the Earth's orbit parameters and the occurrence of reversals (Consolini and De Michelis 2003, Fischer *et al.* 2009) makes it a very interesting subject of geophysics in general.

A few remarks on the homogeneity of dynamo experiments: The Riga dynamo had already a rather high degree of homogeneity, with a length of 3 m along which the flow was susceptible to the back-reacting Lorentz forces resulting from the self-excited magnetic field. Consequently, the saturation curve (i.e., the dependence of the magnetic field energy on the super-criticality) is quite flat (see Figure 5 in Gailitis *et al.* 2008), which reflects the "evasive" character of this fluid dynamo. Nevertheless, two stainless steel tubes were still needed to separate the inner helical flow from the back-flow, and the back-flow from the outer sodium at rest. A significant part of the saturation mechanism relies on the decrease of the differential rotation between down-flow and back-flow (Gailitis *et al.* 2004), which is of course strongly influenced by the presence of a wall. The Karlsruhe experiment contained, for the good reason to show two-scale dynamo action, 52 stainless-steel "spin-generators". Consequently, its saturation curve turned out to be quite steep (again, see Figure 5 in Gailitis *et al.* 2004). The VKS dynamo has shown an impressive variety of dynamical effects such as reversals and excursions (Berhanu *et al.* 2007, Monchaux *et al.* 2009), but only when the impellers were made of soft iron, which compromises significantly its homogeneity. What we are aiming at now is to build a truly homogenous laboratory dynamo that is driven in a near-natural manner.

Despite the motivational background of planetary dynamos working in (near-)spherical geometry, we have opted for a cylindrical geometry due to its stronger, pressure driven forcing of the fluid, for which a wealth of analytical and numerical data exist as well. Much has been learned already about the flow structure in such a setting: when precessing the cylinder very slowly, the initial solid-body rotation is superposed by a non-axisymmetric ($m = 1$) Kelvin mode. Increasing the precession ratio, more modes come into play, until suddenly the quasi-laminar flow gives way to a completely turbulent regime. While the pure hydrodynamics of precession is interesting in itself, and will indeed be studied, the main focus of the experiment will be on the question in which

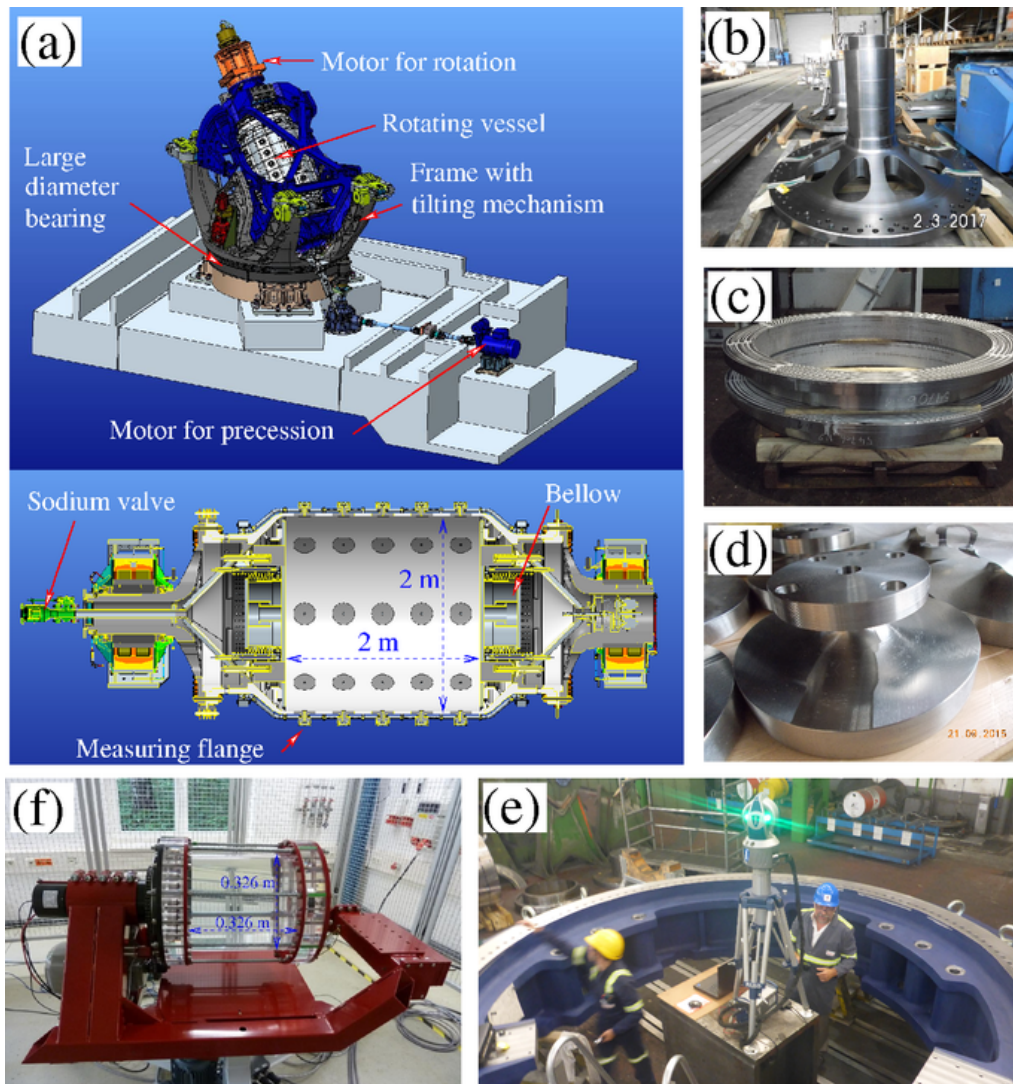


Figure 4: Precession experiment: (a) Design of the entire machine (top) and the central module (bottom). Note that the precession angle can be varied between 45° and 90° (figure courtesy SBS Bühnentechnik GmbH). (b) Photographs of the produced shaft flanges. (c) Two rings of the container. (d) Measuring flanges. (e) Impression from the conformance inspection of the large cast ring to be installed between the ferro-concrete tripod and the large ball bearing. (f) The 1:6 down-scaled water experiment for predicting the flow and pressure fields of the large experiment.

parameter regime dynamo action occurs.

The precession experiment is the most ambitious project within the framework of DRESDYN. The design of the experiment is finalized (see Figure 4a), the construction is ongoing, and first test-experiments with water are expected for 2019. The wealth of results (Herault *et al.* 2015, Giesecke *et al.* 2015, Stefani *et al.* 2017, Giesecke *et al.* 2018, Herault *et al.* 2018), obtained at a 1:6 down-scaled water-dummy experiment (Figure 4f) working up to $Re = 1.5 \times 10^6$, and by numerical simulations up to $Re = 10^4$, provides a sound basis for the large-scale liquid sodium experiment. Since the centrifugal pressure

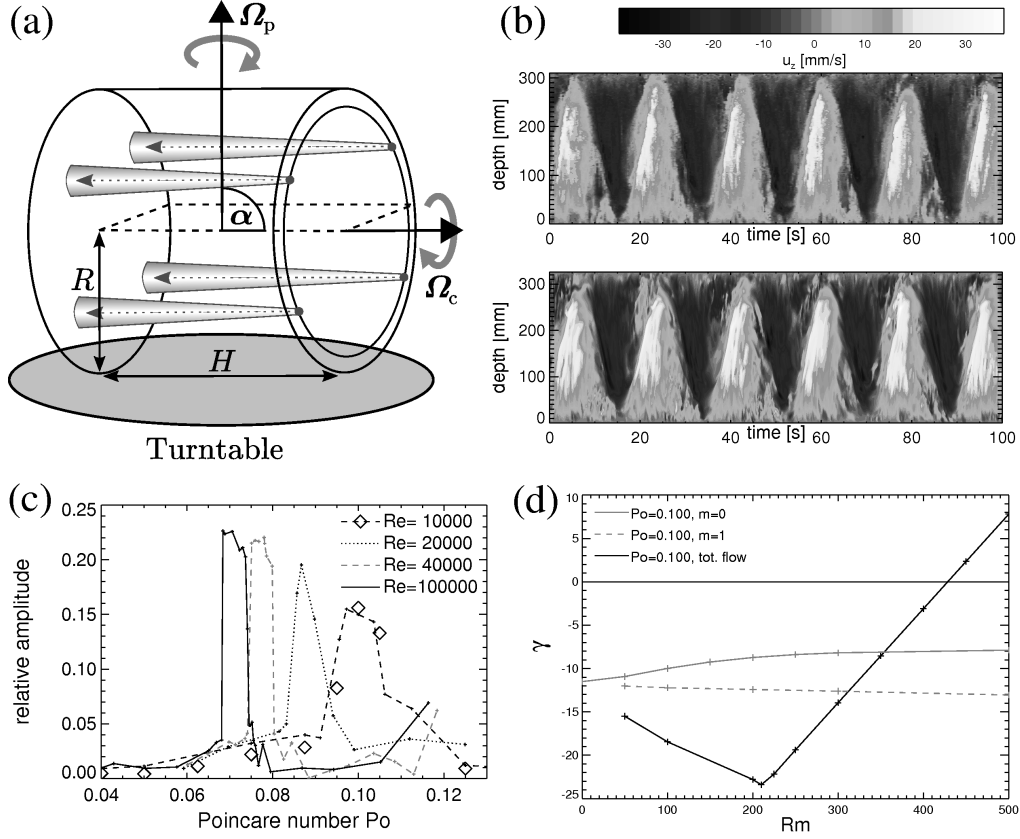


Figure 5: The precession driven flow and its predicted dynamo action. (a) Scheme of the down-scaled water experiment (see Figure 4f) with 4 Ultrasonic Doppler Velocity (UDV) transducers for flow measurement. (b) Temporal evolution of the axial velocity $u_z(z, t)$ at a radius $r = 150$ mm (upper panel: UDV measurements, lower panel: simulations). (c) Relative amplitude of the axisymmetric double-roll mode with respect to the dominant $m = 1$ mode for various Re . The curves denote results from the water experiment, and the diamonds denote results from simulations. (d) Growth rates of the dynamo-generated magnetic field versus Rm for combinations of various azimuthal modes from the velocity field obtained at simulations at $Re = 10^4$ and $Po = 0.1$. The vertical dashed lines indicate the respective dynamo thresholds. The full flow leads to a critical $Rm = 428$ (after Giesecke *et al.* 2018).

(up to 20 bar), in combination with the precession-driven pressure swing (up to 10 bar) (Stefani *et al.* 2017), make the safe construction of the cylindrical shell a great challenge, the first water experiments will serve for confirming the ultimately allowable rotation and precession rates which by now are supposed to be 10 Hz and 1 Hz, respectively.

As for the dynamo action of the precession-driven flow, we have recently obtained a very promising result (Giesecke *et al.* 2018) which helps constraining the parameter regime to be explored (Figure 5). This result relies on the numerical and experimental finding that, shortly before the transition from the laminar to the turbulent flow, the non-linear self-interaction of the dominant forced $m = 1$ Kelvin mode produces an axisymmetric ($m = 0$) mode with doubled axial wavenumber (Figure 5c). The resulting

double-roll structure is known to be an efficient dynamo (Dudley and James 1983). Indeed, numerical dynamo simulations have shown a critical magnetic Reynolds number of $Rm_c = 428$ (Figure 5d), which is safely below the experimentally achievable value of $Rm = 700$. Despite some remaining ambiguities, concerning the scaling with the Reynolds number and the detailed role of electrical boundary conditions, this double-roll mode has been experimentally shown to be a robust phenomenon, which seems also be linked to the hysteretic behaviour of the laminar/turbulent transition as observed previously (Herault *et al.* 2015). Hence, one might indeed be optimistic to find dynamo action close to a precession ratio of $Po := f_{\text{prec}}/f_{\text{cyl}} \approx 0.06$, and at around 2/3 of the available rotation speed. Further to this, it is also planned to explore the turbulent regime, for which neither the flow structure nor its dynamo action is well understood. While we expect a significant amount of small-scale helicity to build up in this regime, it could be possible that its dynamo capability is thwarted by the simultaneous increase of the turbulent resistivity (β -effect), an effect that might have played a detrimental role in previous experimental dynamo studies (Rahbarnia *et al.* 2012).

3.2 MRI/TI experiment

The aim of the combined MRI/TI experiment is two-fold: First, we want to study in detail the transition between the helical MRI (HMRI) and the standard MRI (SMRI), by simultaneously increasing the Reynolds and Hartmann numbers and decreasing the ratio of azimuthal to axial field (Hollerbach and Rüdiger 2005). The relation between SMRI and HMRI, in particular with respect to the scaling behaviour, has spurred a lot of theoretical and numerical activities. The continuous transition between them relies on the formation of an exceptional point at which the slow magneto-Coriolis wave and the inertial wave coalesce and exchange their branches (Kirillov and Stefani 2010). In order to see this transition in experiment we have to go from $Re \sim 10^3$ and $Ha \sim 10$ to $Re \sim 10^6$ and $Ha \sim 10^3$. The Princeton experiment had proved the demonstration of SMRI to be extremely challenging for the simple reason that purely hydrodynamic flows with $Re \sim 10^6$, when axially bounded, are extremely hard to keep stable, whatever linear stability analysis for Taylor-Couette flows with infinite length tells us. The provision of a central current in our experiment has the crucial advantage that we can start from the well-known regime of HMRI, and approach from there the SMRI regime in a continuous manner.

The second goal is to study various combinations of AMRI (or HMRI) with TI by guiding additional currents through the liquid. As revealed recently (Kirillov and Stefani 2013, Kirillov *et al.* 2014, Rüdiger *et al.* 2015), this combination allows to destabilize even Keplerian profiles at very moderate values of Re and Ha , which was not possible in the HMRI and AMRI experiments at PROMISE with its purely central current through the hole (Stefani *et al.* 2006, Seilmayer *et al.* 2014).

The construction of the liquid-sodium MRI/TI experiment (Figure 6) relies on our experience with HMRI and AMRI gained at the PROMISE facility, and with the TI experiment. One of the main constructional challenges of the new device is to combine a sophisticated mechanical configuration of split end-rings (which is necessary for the MRI part) with appropriate electrical contacts for applying the internal currents that are needed for the TI. As shown by Rüdiger *et al.* (2003), MRI for liquid sodium starts at a magnetic

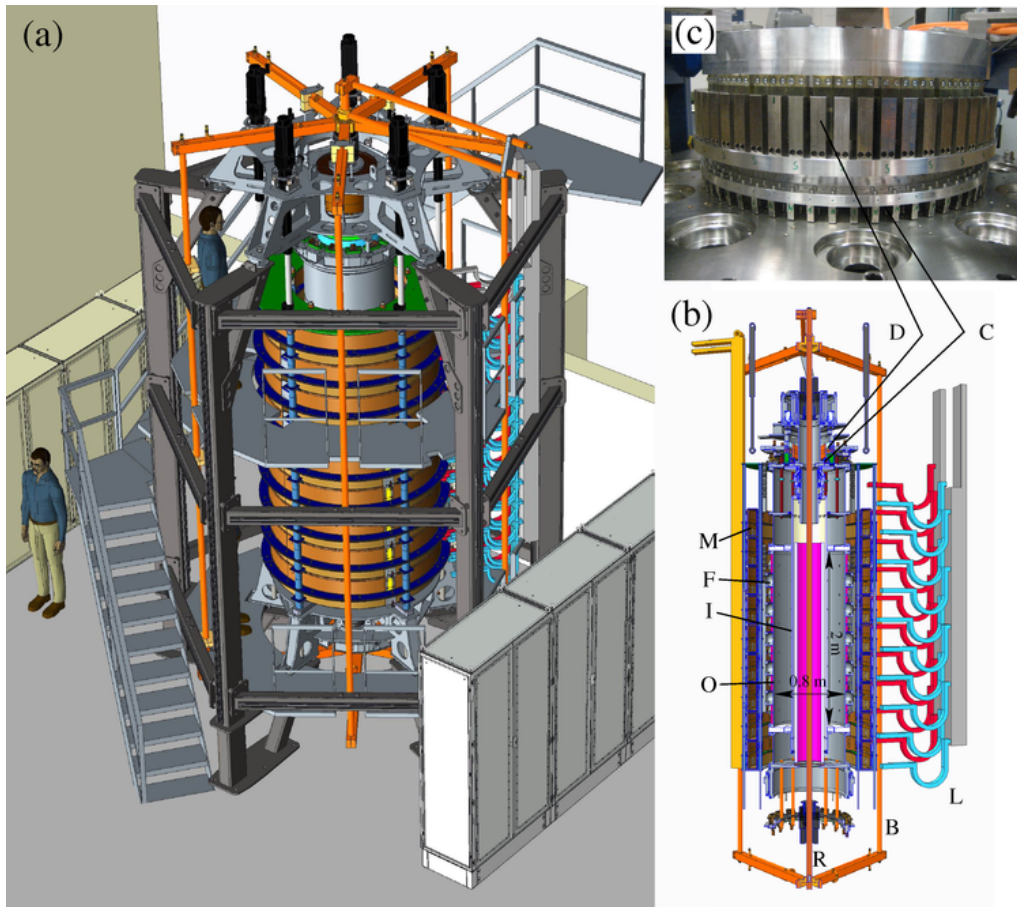


Figure 6: The liquid sodium experiment for the combined investigation of MRI and TI. (a) Drawing of the entire facility. (b) Drawing of the central module: I- Inner cylinder, O - Outer cylinder, F - Measurement flanges, M - Magnet for the axial field, R - Central rod for the azimuthal field, B - Back-wires for return current, D - Drive for the inner cylinder, C - Magnetic coupler for the inner cylinder (figure courtesy S. Köppen). (c) Photograph of the drive and the magnetic coupler.

Reynolds number of $Rm = 21$ and a Lundquist number of $Lu = 4.4$ (both values correspond to the more conservative estimate for different electrical boundary conditions). With a height of the active Taylor-Couette cell of 2 m (Figure 2b), and an outer radius of 0.4 m, we plan to reach a rotation rate of the inner cylinder of 20 Hz and an axial field of 130 mT, which is in either case more than double the critical value. With view on the safety issues when dealing with one ton of liquid sodium, one of the most critical aspects is the driving of the inner cylinder. For that purpose, a sophisticated magnetic coupler (Figure 6c) has been developed and already tested, which ensures a hermetic seal of the entire experiment. Another critical part of the experiment is the large coil for generating the axial magnetic field. Great effort was spent to make this field as homogeneous as possible. The resulting construction weighs 5 tons, and will require around 120 kW of electrical power.

First experiments are planned for 2020. For the sake of its overwhelming scientific relevance, we will first try to approach standard MRI from the well-known regime of heli-

cal MRI. The procedure to do so was already indicated in the original paper by Hollerbach and Rüdiger (2005) where the optimal parameters for transition between HMRI and SMRI were determined. The study of combinations of AMRI and HMRI with TI is planned for a later stage of the experiment. In addition to the currents through the central rod, for the TI part we will also need currents through the liquid. In the foreseen geometry with a ratio of inner to outer radius of 0.5, the Tayler instability will set in at around 1 kA for non-rotating cylinders. For rotating cylinders this number increases according to Rüdiger and Schulz (2010).

3.3 Super-AMRI

As shown recently, both in the framework of a short-wavelength approximation (Stefani and Kirillov 2015) and by a 1D-stability code (Rüdiger *et al.* 2016, Rüdiger *et al.* 2018a), a conducting fluid with very strong positive shear might develop an $m = 1$ instability ("Super-AMRI") when subjected to an azimuthal magnetic field. Similar effects occur, for optimized ratios of azimuthal to axial field, also for other azimuthal wavenumbers, including $m = 0$ ("Super-HMRI"). This surprising result becomes plausible when relating the growth rate of HMRI with the non-modal growth factor of purely hydrodynamic flows, which leads to a very simple and nearly linear relationship (Mamatsashvili and Stefani 2016). As a brief astrophysical digression: given the rather small magnetic Prandtl number of the solar tachocline (10^{-3} - 10^{-2}), which is actually not that far from those of liquid metals (10^{-6} - 10^{-5}), we expect to gain new insight into the dynamics of its equator-near parts which exhibit indeed positive shear, with possible consequences for our alternative model of the solar dynamo (Stefani *et al.* 2016b).

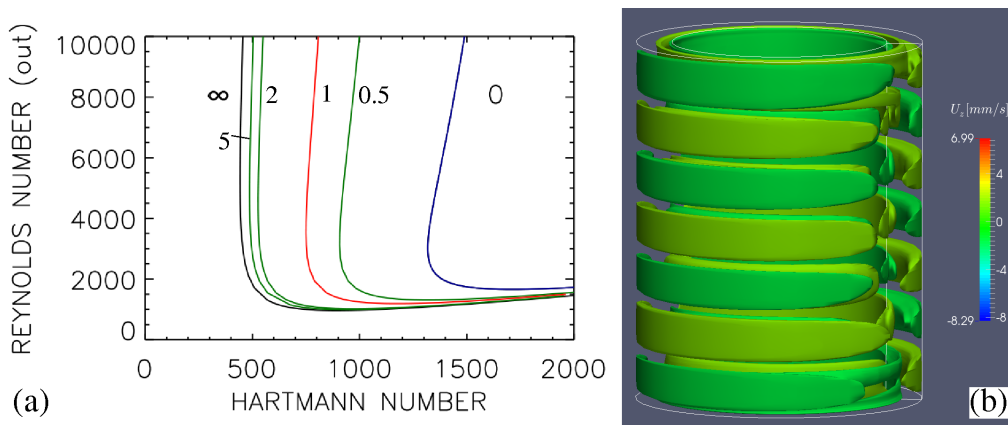


Figure 7: Numerical simulations for the Super-AMRI experiment. (a) Stability threshold in dependence on Ha and Re for a radius ratio $r_i/r_o = 0.9$. The numbers in the plot indicate the assumed ratio of wall conductivity to fluid conductivity. A ratio of 5, which correspond approximately to a copper wall for liquid sodium, is close to the limit of infinite wall conductivity. (b) Simulated axial velocity perturbation for $r_i/r_o = 0.75$ (Figure courtesy to M. Gellert).

While the critical Reynolds number for Super-AMRI is only a few thousand, which presents no problem for a respective experiment, the predicted critical values of the cen-

tral current range from 25 to 80 kA, depending strongly on the electrical boundary conditions. This is indeed a critical point, even under the assumption that a current source of 50 kA will be available for the combined MRI/TI experiment. Very recent numerical simulations, taking into account realistic combinations of the conductivities of the fluid (sodium) and the wall (copper, for example), had revealed a technical optimum of around 33 kA for a ratio of inner to outer cylinder radii of $r_i/r_o = 0.78$ (Rüdiger *et al.* 2018b).

A corresponding Super-AMRI experiment is still in its conceptual phase. Assuming the radii ratio to be as small as 0.75, as in Figure 7b, then a certain minimum of the Taylor-Couette gap will be approximately 3 cm, which is needed for the UDV sensors to distinguish between up- and down-flowing fluid parcels. This value would translate to a minimum radius of the experiment of 12 cm. Further optimization will definitely be needed here. It remains also to be tested whether the central current can still be reduced for a corresponding Super-HMRI experiment.

4 Conclusions and prospects

In this short review, we have delineated the progress in the experimental investigation of the dynamo effect and of magnetically triggered flow instabilities that was gained during the last two decades. With the DRESDYN project, we plan to continue this research programme by showing dynamo action in a homogenous fluid driven by precession, and by approaching standard MRI in a Taylor-Couette experiment. Additional experiments on the magnetic destabilization of positive shear flows are also planned. While having focused on liquid metal experiments, we see also a huge potential for corresponding plasma experiments which have the great advantage of allowing to adjust the magnetic Prandtl number, and whose scientific exploitation has just begun (Forest *et al.* 2015, Weisberg *et al.* 2017).

Acknowledgments

We thank Bernd Wustmann, Christian Steglich, Frank Herbrand, and Sebastian Köppen for their technical assistance in the design and construction of various experiments. The long-standing collaboration with Marcus Gellert, Rainer Hollerbach, Oleg Kirillov, George Mamatsashvili and Manfred Schultz is gratefully acknowledged.

References

Avalos-Zuñiga, R.A., Priede, J. and Bello-Morales, C.E., A homopolar disk dynamo experiment with liquid metal contacts. *Magnetohydrodynamics* 2017, **53**, 341-347.

Balbus, S.A., Enhanced angular momentum transport in accretion disks. *Ann. Rev. Astron. Astrophys.* 2003, **41**, 555-597.

Balbus, S.A. and Hawley, J.F., A powerful local shear instability in weakly magnetized disks. 1. Linear Analysis. *Astrophys. J.* 1991, **376**, 214-221.

Berhanu, M. *et al.*, Magnetic field reversals in an experimental turbulent dynamo. *EPL* 2007, **77**, 59001.

Consolini, G. and De Michelis, P., Stochastic resonance in geomagnetic polarity reversals. *Phys. Rev. Lett.* 2003, **90**, 058501.

Colgate, S.A. *et al.*, High magnetic shear gain in a liquid sodium stable Couette flow experiment: A prelude to an $\alpha - \Omega$ dynamo. *Phys. Rev. Lett.* 2011, **106**, 175003

Dudley, M.L. and James, R.W., Time-dependent kinematic dynamos with stationary flows. *Proc. R. Soc. A* 1989, **425**, 407-429.

Dwyer, C.A., Stevenson, D.J. and Nimmo, F., A long-lived lunar dynamo driven by continuous mechanical stirring. *Nature* 2012, **220** 47-61.

Fischer, M., Gerbeth, G., Giesecke, A. and Stefani, F., Inferring basic parameters of the geodynamo from sequences of polarity reversals. *Inverse Probl.* 2009, **25** 065011.

Forest, C.B. *et al.*, The Wisconsin plasma astrophysics laboratory. *J. Plasma Phys.* 2015, **81**, 345810501.

Frick, P. *et al.*, Direct measurement of effective magnetic diffusivity in turbulent flow of liquid sodium. *Phys. Rev. Lett.* 2010, **105**, 184502

Fu, R.R. *et al.*, An ancient core dynamo in asteroid Vesta. *Science* 2013, **338**, 238-241.

Gailitis, A., Theory of the Herzenberg dynamo. *Magnetohydrodynamics* 1973, **9**, 445-449.

Gailitis, A. and Freibergs, Ya., Theory of a helical MHD dynamo. *Magnetohydrodynamics* 1976, **12**, 127-129.

Gailitis, A. *et al.*, Experiment with a liquid-metal model of an MHD dynamo. *Magnetohydrodynamics* 1987, **23**, 349-353.

Gailitis, A. *et al.*, Detection of a flow induced magnetic field eigenmode in the Riga dynamo facility. *Phys. Rev. Lett.* 2000, **84**, 4365-4369.

Gailitis, A. *et al.*, Magnetic field saturation in the Riga dynamo experiment. *Phys. Rev. Lett.* 2001, **86**, 3024-3027.

Gailitis, A., Lielausis, O., Platācis, E., Gerbeth, G. and Stefani, F., Laboratory experiments on hydromagnetic dynamos. *Rev. Mod. Phys.* 2002, **74**, 973-990.

- Gailitis, A., Lielausis, O., Platacis, E., Gerbeth, G. and Stefani, F., The Riga dynamo experiment. *Surv. Geophys.* 2003, **24**, 247-267.
- Gailitis, A., Lielausis, O., Platacis, E., Gerbeth, G. and Stefani, F., Riga dynamo experiment and its theoretical background. *Phys. Plasmas* 2004, **11**, 2838-2843.
- Gailitis, A., Gerbeth, G., Gundrum, Th., Lielausis, O., Platacis, E. and Stefani, F., History and results of the Riga dynamo experiments. *C.R. Phys.* 2008, **9**, 721-728.
- Gailitis, A. and Lipsbergs, G., 2016 year experiments at Riga dynamo facility, *Magneto-hydrodynamics* 2017, **53**, 349-356.
- Gailitis, A., Gerbeth, G., Gundrum, Th., Lielausis, O., Lipsbergs, G., Platacis, E. and Stefani, F., Self-excitation in a helical liquid metal flow: The Riga dynamo experiments. *J. Plasma Phys.* 2018, submitted; arXiv:1801.01749.
- Gans, R.F., On hydromagnetic precession in a cylinder. *J. Fluid Mech.* 1970, **45**, 111–130.
- Giesecke, A., Stefani, F. and Gerbeth, G., Role of soft-iron impellers on the mode selection in the von Kármán-sodium dynamo experiment. *Phys. Rev. Lett.* 2010, **104**, 044503.
- Giesecke, A. *et al.*, Influence of high-permeability discs in an axisymmetric model of the Cadarache dynamo experiment. *New J. Phys.* 2012, **14**, 053005.
- Giesecke, A. *et al.*, Triadic resonances in nonlinear simulations of a fluid flow in a precessing cylinder. *New J. Phys.* 2015, **17**, 113044.
- Giesecke, A., Vogt, T., Gundrum, T. and Stefani, F., Nonlinear large scale flow in a precessing cylinder and its ability to drive dynamo action. *Phys. Rev. Lett.*, 2018 **120**, 024502.
- Goepfert, O. and Tilgner, A., Dynamos in precessing cubes. *New J. Phys.* 2016, **18**, 103019.
- Goto, S., Shimizu, M. and Kawahara, G., Turbulent mixing in a precessing sphere. *Phys. Fluids* 2014, **26**, 115106.
- Herault, J., Gundrum, T., Giesecke, A. and Stefani, F., Subcritical transition to turbulence of a precessing flow in a cylindrical vessel. *Phys. Fluids* 2015, **27**, 124102.
- Herault, J., Giesecke, A., Gundrum, T. and Stefani, F., Instability of precession driven Kelvin modes: evidence of a detuning effect. *Phys. Rev. F* 2018, submitted.
- Herzenberg, A., Geomagnetic dynamos. *Philos. Trans. R. Soc. Lond.* 1958, **A250**, 543–

585.

Hollerbach, R. and Rüdiger, G., New type of magnetorotational instability in cylindrical Taylor-Couette flow. *Phys. Rev. Lett.* 2005, **95**, 124501.

Hollerbach, R., Teeluck, V. and Rüdiger, G., Nonaxisymmetric magnetorotational instabilities in cylindrical Taylor-Couette flow. *Phys. Rev. Lett.* 2010, **104**, 044502.

Hollerbach, R. *et al.*, Electromagnetically driven zonal flows in a rapidly rotating spherical shell. *J. Fluid Mech.* 2013, **725**, 428-445.

Kerswell, R.R., The instability of precessing flow. *Geophys. Astrophys. Fluid Dyn.* 1993, **72**, 107-144.

Kirillov, O.N. and Stefani, F., On the relation of standard and helical magnetorotational instability. *Astrophys. J.* 2010, **712**, 52-68.

Kirillov, O.N. and Stefani, F., Extending the range of inductionless magnetorotational instability. *Phys. Rev. Lett.* 2013, **111**, 061103.

Kirillov, O.N., Stefani, F. and Fukumoto, Y., Local instabilities in magnetized rotational flows: a short-wavelength approach. *J. Fluid Mech.* 2014, **760**, 591-633.

Kreuzahler, S., Ponty, Y., Plihon, N., Homann, H. and Grauer, R., Dynamo enhancement and mode selection triggered by high magnetic permeability. *Phys. Rev. Lett.* 2017, **119**, 234501.

Lagrange, R., Eloy, C., Nadal, F. and Meunier, P., Instability of a fluid inside a precessing cylinder. *Phys. Fluids* 2008, **20**, 081701.

Lathrop, D.P. and Forest, C.B., Magnetic dynamos in the lab. *Phys. Today* 2011, **64**(7), 40-45.

Lin, Y., Marti, P. and Noir, J., Shear-driven parametric instability in a precessing sphere. *Phys. Fluids* 2015, **27**, 046601.

Liu, W., Goodman, J. and Ji, H., Simulations of magnetorotational instability in a magnetized Couette flow. *Astrophys. J.* 2006a, **643**, 306-317.

Liu, W., Goodman, J., Herron, I. and Ji, H., Helical magnetorotational instability in magnetized Taylor-Couette flow. *Phys. Rev. E* 2006b, **643**, 056302.

Lowes, F.J. and Wilkinson, I., Geomagnetic dynamo - A laboratory model. *Nature* 1963, **198**, 1158-1160.

- Lowes, F.J. and Wilkinso, I., Geomagnetic dynamo - An improved laboratory model. *Nature* 1963, **219**, 717-718.
- Malkus, W.V.R., Precession of Earth as cause of geomagnetism. *Science* 1968, **160**, 259-264.
- Mamatsashvili, G. and Stefani, F., Linking dissipation-induced instabilities with non-modal growth: The case of helical magnetorotational instability. *Phys. Rev. E* 2016, **94**, 051203.
- Miralles, S. *et al.*, Dynamo threshold detection in the von Kármán sodium experiment. *Phys. Rev. Lett.* 2013, **88**, 013992.
- Monchaux, R. *et al.*, Generation of a magnetic field by dynamo action in a turbulent flow of liquid sodium. *Phys. Rev. Lett.* 2007, **98**, 044502.
- Monchaux, R. *et al.*, The von Kármán sodium experiment: Turbulent dynamical dynamos. *Phys. Fluids* 2009, **21**, 035108.
- Mouhali, W., Lehner, T., Léorat, J. and Vitry, R. Evidence for a cyclonic regime in a precessing cylindrical container. *Exp. Fluids* 2012, **53**, 1693-1700.
- Müller and Stieglitz, R., Can the Earth's magnetic field be simulated in the laboratory? *Naturwissenschaften* 2000, **87**, 381-390.
- Müller, U. and Stieglitz, R., The Karlsruhe dynamo experiment. *Nonl. Proc. Geophys.* 2002, **9**, 165-170.
- Müller, U., Stieglitz, R. and Horanyi, S., A two-scale hydromagnetic dynamo experiment. *J. Fluid Mech.* 2004, **498**, 31-71.
- Noir, J. and Cebbron, D, Precession-driven flows in non-axisymmetric ellipsoids. *J. Fluid Mech.* 2013, **737**, 412-439.
- Nore, C., Léorat, J., Guermond, J.-L. and Luddens, F., Nonlinear dynamo action in a precessing cylindrical container. *Phys. Rev. E* 2011, **84**, 016317.
- Nore, C., Quiroz, D.C., Capanera, L. and Guermond, J.-L., Direct numerical simulation of the axial dipolar dynamo in the von Kármán Sodium experiment. *EPL* 2016, **14**, 65002.
- Nornberg, M.D., Ji, H., Schartman, E., Roach, A., and Goodman, J., Observation of magnetocoriolis waves in a liquid metal Taylor-Couette experiment. *Phys. Rev. Lett.* 2010, **104**, 074501.
- Ponomarenko, Y.B., On the theory of hydromagnetic dynamos, *Zh. Prikl. Mekh. & Tekh.*

Fiz. (USSR) 1973, **6**, 47-51.

Rädler, K.-H., Apstein, E., Rheinhardt, M. and Schüler, M., The Karlsruhe dynamo experiment. A mean field approach. *Stud. Geophys. Geodaet.* 1998, **42**, 224-231.

Rädler, K.-H., Rheinhardt, M., Apstein, E. and Fuchs, H., On the mean-field theory of the Karlsruhe dynamo experiment. *Nonlin. Proc. Geophys.* 2002, **9**, 171-187.

Rahbarnia, K. *et al.*, Direct observation of the turbulent emf and transport of magnetic field in a liquid sodium experiment. *Astrophys. J.* 2012, **759**, 80.

Roach, A. *et al.*, Observation of a free-Shercliff-layer instability in cylindrical geometry. *Phys. Rev. Lett.* 2012, **108**, 154502.

Rüdiger, G., Schultz, M and Shalybkov, D., Linear magnetohydrodynamic Taylor-Couette instability for liquid sodium. *Phys. Rev. E* 2003, **67** 046312.

Rüdiger, G., Hollerbach, R., and Kitchatinov, L.L., *Magnetic processes in astrophysics: theory, simulations, experiments*, 2013 (Weinheim: WILEY-VCH).

Rüdiger, G., Schultz, M., Stefani, F. and Mond, M., Diffusive magnetohydrodynamic instabilities beyond the Chandrasekhar theorem. *Astrophys. J.* 2015, **811**, 84.

Rüdiger, G., Schultz, M., Gellert, M. and Stefani, F., Subcritical excitation of the current-driven Tayler instability by super-rotation. *Phys. Fluids* 2016, **28**, 014105.

Rüdiger, G., Schultz, M., Gellert, M. and Stefani, F., Azimuthal magnetorotational instability with super-rotation. *J. Plasma Phys.* 2018, **84**, 735840101.

Rüdiger, G., Schultz, M., Stefani, F. and Hollerbach, R., Magnetorotational instability in Taylor-Couette flows between cylinders with finite electrical conductivity. *Geophys. Astrophys. Fluid Dyn.* 2018, submitted.

Schmitt, D. *et al.*, Magneto-Coriolis waves in a spherical Couette flow experiment. *Eur. J. Mech. - B/Fluids* 2013, **37**, 10-22.

Seilmayer, M. *et al.*, Experimental evidence for a transient Tayler instability in a cylindrical liquid-metal column. *Phys. Rev. Lett.* 2012, **108**, 244501.

Seilmayer, M. *et al.*, Experimental evidence for nonaxisymmetric magnetorotational instability in a rotating liquid metal exposed to an azimuthal magnetic field. *Phys. Rev. Lett.* 2014, **113**, 024505.

Sisan, D.R. *et al.*, Experimental observation and characterization of the magnetorotational instability. *Phys. Rev. Lett.* 2004, **93**, 114502.

Shalimov, S.L., On effect of precession-induced flows in the liquid core for early Earth's history. *Nonl. Proc. Geophys.* 2006, **13**, 525-529.

Spence, E.J. *et al.*, Observation of a turbulence-induced large scale magnetic field. *Phys. Rev. Lett.* 2006, **96**, 055002.

Spruit, H.C., Dynamo action by differential rotation in a stably stratified stellar interior. *Astron. Astrophys.* 2002, **381**, 923-932.

Steenbeck, M. *et al.*, Der experimentelle Nachweis einer elektromotorischen Kraft längs eines äußeren Magnetfeldes, induziert durch eine Strömung flüssigen Metalls (α -Effekt). *Mber. Dtsch. Akad. Wiss. Berl.* 1967, **9**, 714-719.

Stefani, F., Gerbeth, G. and Gailitis, A., Velocity profile optimization for the Riga dynamo experiment. In *Transfer Phenomena in Magnetohydrodynamic and electroconducting Flows*, edited by A. Alemany, Ph. Marty and J.-P. Thibault, pp. 31-44, 1999 (Kluwer: Dordrecht).

Stefani, F. *et al.*, Experimental evidence for magnetorotational instability in a Taylor-Couette flow under the influence of a helical magnetic field. *Phys. Rev. Lett.* 2006, **97**, 184502.

Stefani, F. *et al.*, Experiments on the magnetorotational instability in helical magnetic fields. *New J. Phys.* 2007, **9**, 295.

Stefani, F., Gailitis, A. and Gerbeth, G., Magnetohydrodynamic experiments on cosmic magnetic fields. *Zeitschr. Angew. Math. Mech.* 2008, **88**, 930-954.

Stefani, F. *et al.*, Helical magnetorotational instability in a Taylor-Couette flow with strongly reduced Ekman pumping. *Phys. Rev. E* 2009, **80**, 066303.

Stefani, F. *et al.*, DRESHDYN - A new facility for MHD experiments with liquid sodium. *Magnetohydrodynamics* 2012, **48**, 103-114.

Stefani, F. and Kirillov, O.N., Destabilization of rotating flows with positive shear by azimuthal magnetic fields. *Phys. Rev. E* 2015, **92**, 051001(R).

Stefani, F. *et al.*, Towards a precession driven dynamo experiment. *Magnetohydrodynamics* 2015, **51**, 275-284.

Stefani, F. *et al.*, Magnetohydrodynamic effects in liquid metal batteries. *IOP Conf. Ser.: Mater. Sci. Eng.* 2016a, **143**, 012024.

Stefani, F., Giesecke, A., Weber, N. and Weier, T. Synchronized helicity oscillations: A

- link between planetary tides and the solar cycle? *Solar Phys.* 2016b, **291**, 2197-2212.
- Stieglitz R. and Müller U., Experimental demonstration of a homogeneous two-scale dynamo. *Phys. Fluids* 2001, **13**, 561-564.
- Szklarski, J., Reduction of boundary effects in the spiral MRI experiment PROMISE. *Astron. Nachr.* 2007, **328**, 499-506.
- Tayler, R.J., Adiabatic stability of stars containing magnetic fields. 1. Toroidal fields. *Mon. Not. R. Astron. Soc.* 1973, **161**, 365-380.
- Tilgner, A. Numerical simulation of the onset of dynamo action in an experimental two-scale dynamo. *Phys. Fluids* 2002, **14**, 4092-4094.
- Tilgner, A., Precession driven dynamos. *Phys. Fluids* 2005, **17**, 034104.
- Tilgner, A., Kinematic dynamos with precession driven flow in a sphere. *Geophys. Astrophys. Fluid Dyn.* 2007, **101**, 1-9.
- Vanyo, P. and Dunn, J.R., Core precession: flow structures and energy. *Geophys. J. Int.* 2000, **142**, 409-425.
- Velikhov, E.P, Stability of an ideally conducting liquid flowing between cylinders rotating in a magnetic field. *Sov. Phys. JETP* 1959, **36**, 995-998.
- Weisberg, D.B. *et al.*, Driving large magnetic Reynolds number flow in highly ionized, unmagnetized plasmas. *Phys. Plasmas* 2017, **24**, 056502.
- Weiss, B.P. and Tikoo, S.M., The lunar dynamo. *Science* 2014, **346**, 1246753.
- Wilkinson, I., The contribution of laboratory dynamo experiments to our understanding of the mechanism of generation of planetary magnetic fields. *Geophys. Surveys* 1984, **7**, 107-122.
- Wondrak, T. *et al.*, Contactless inductive flow tomography for a model of continuous steel casting. *Meas. Sci. Techn.* 2010, **21**, 045402.
- Wu, C.C. and Roberts, P.H., On a dynamo driven by topographic precession. *Geophys. Astrophys. Fluid Dyn.* 2009, **103**, 467-501.
- Zimmermann, D.S., Triana, S.A., Nataf, H.-C. and Lathrop, D.P., A turbulent, high magnetic Reynolds number experimental model of Earth's core. *J. Geophys. Res. - Sol. Earth* 2010, **119**, 4538-4557